31st Annual International Conference of the IEEE EMBS
Minneapolis, Minnesota, USA, September 2-6, 2009

Multi-space clustering for segmentation of exudates in retinal color photographs

Keerthi Ram and Jayanthi Sivaswamy

Abstract— **Exudates are a class of lipid retinal lesions visible through optical fundus imaging, and indicative of diabetic retinopathy. We propose a clustering-based method to segment exudates, using multi-space clustering, and colorspace features. The method was evaluated on a set of 89 images from a publicly available dataset, and achieves an accuracy of 89.7% and positive predictive value of 87%.**

I. INTRODUCTION

Diabetic retinopathy (DR) is a sight-threatening risk inflicting diabetic patients. Exudates are a class of lipid lesions visible in optical retinal images, which are clinical signs of DR. Two manifestations of exudates are known: hard exudates, that appear as bright yellow regions, and soft exudates or cotton-wool spots, which have fuzzy appearance. Automatic detection of exudates is of interest as it can assist ophthalmologists in DR diagnosis and early treatment.

The common approaches to lesion-level exudate detection follow a bottom-up strategy [1], beginning with pixel classification, followed by region-level classification. Color values are used in pixel classification, since exudate pixels exhibit a limited range of color. Region-level classification has been attempted with features like edge-strength [1], mean intensity within the region [2], [3], and contrast features [4]. The optic disk is a structure with similar color characteristics as exudates, imaged in the central views of the retina. Optic disk has been distinguished by using entropy features [5], or using dedicated methods like active contours [6].

Existing work use supervised classification like k-nearest neighbor [4], neural networks or SVM [1]. In these methods, color normalization is performed as a common step in order to reduce the variability within retinal images, occuring due to imaging conditions, pigmentation, and presence of other pathology. Color is a prominent characteristic of exudates, and the performance of existing approaches rely on the ability of the normalization technique to handle the variability effectively.

Segmentation may also be performed in an unsupervised manner. Low-level segmentation has been performed by clustering using multispectral images and uniform-sized neighborhoods [7]. To achieve segmentation using clustering, features are computed at each pixel (or its neighborhood), thereby yielding data points in feature space. The clustering algorithm then assigns labels to each data point by optimizing over a cost function [1], [2], [6]. Segments are contiguous regions of pixels receiving the same label.

The authors are with the Centre for Visual Information Technology, International Institute of Information Technology-Hyderabad, India keerthiram@research.iiit.ac.in

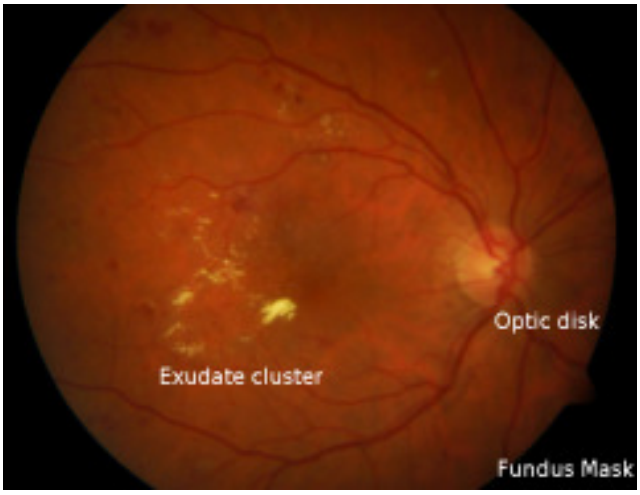

Fig. 1. Retinal image indicating an exudate cluster, optic disk and the fundus mask

Two factors play a role in the clustering method: the feature space used, and the distance metric defined upon that space. The cost function uses the distance metric to find the proximity of cluster prototypes to each pixel, and assigns labels based on optimal values of the cost function.

Multi-space clustering is a technique which uses multiple feature spaces, with potentially each feature space using a different clustering algorithm and distance metric [8]. This technique has shown improvement in performance compared to single-space clustering [8], [9]. The improvement is achieved by coercing the outcomes of the individual clusterings in a constrained fashion.

In this work, we propose a multi-space clustering approach to exudate segmentation, which does not use color normalization or preprocessing. The proposed method uses colorspace features constituting two feature spaces. Clustering is performed individually in each feature space, and the obtained labels are combined in a special manner to yield exudate segments.

II. PROPOSED METHOD

The proposed method is a bottom-up approach consisting of the following steps:

1) suppressing the fundus mask
2) obtaining pixel values in multiple color spaces
3) constructing the feature spaces to perform clustering
4) clustering to obtain labels
5) combining the clustering outcomes, to get candidate regions

978-1-4244-3296-7/09/$25.00 ©2009 IEEE

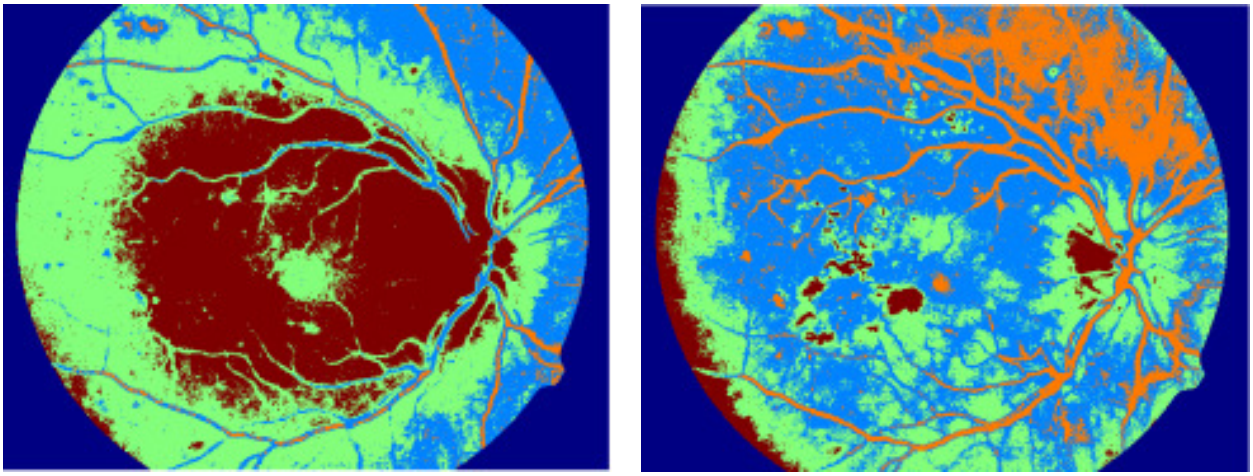

(a) Clustering in $\mathbf{f_1}$ (b) Clustering in $\mathbf{f_2}$

Fig. 2. Clustering based segmentation in two feature spaces

6) suppressing false candidates

The fundus mask is the dark peripheral part of the RGB retinal image, which does not contain informative pixels (fundus pixels). The fundus mask can be excluded by thresholding the brightness (V of HSV space). The next step computes color transformations into four color spaces, for each of the fundus pixels. Conditionally independent feature spaces are constructed from the colorspace values. We have considered the following colorspaces: RGB, CIE L*u*v*, HSV, HSI, and constructed two feature spaces: $\mathbf{f_1}$: (H, S, V, I) , and $\mathbf{f_2}$: $(R, G, L*, u*, v*)$. It can be seen that conditional independence is ensured among the two feature spaces. This is essential [8] for the multi-space clustering framework.

We use k-means clustering, $1-$cross-correlation being the distance metric, treating data points as sequences. The values forming each such sequence are normalized to have zero mean and unit standard deviation. The clusters are initialized by performing a preliminary clustering with random 10% subsampling of the data, and k centroids at random. We set $k = 4$, thereby partitioning the image into 4 segments.

Clustering in $\mathbf{f_1}$ results in segments corresponding to the following structures in the retinal image:

1) Bright lesions and bright background
2) Vessels, dark background, macula region
3) General retinal background
4) Peripheral region,

whereas clustering in $\mathbf{f_2}$ results in the following segmentation:

1) Optic disk, hard exudates, peripheral bright regions
2) Vessels, dark lesions, dark background
3) Regions surrounding the bright objects (enclosing regions of (1))
4) Other background pixels

Regions of $\mathbf{f_1}$ with label 1 (denote $L_1.1$) miss some minute, isolated exudates and some faint exudates, which are however picked up in $\mathbf{f_2}$ label 1 (denote $L_2.1$), at the cost of picking several periphery pixels. The choice of feature space has yielded this complementary nature to the clustering relevant to the region of interest. The labels, if combined appropriately, help to maximally identify the exudate regions and optic disk. We subsequently show a scheme devised to achieve this.

Clustering results in separation of the four clusters, from which we identify the cluster corresponding to $L_1.1$ and $L_2.1$ using the following observations:

1) exudates are bright lesions: $\max(I)$ value (of HSI) will be high in the exudate cluster.
2) exudates exhibit a yellowish color: $\max(R) - \max(G)$ in exudate cluster should have a low value.
3) cluster having minimum $\max(I)$ can be rejected as being $L_1.2$ or $L_2.2$. Similarly cluster having maximum $\max(R) - \max(G)$ can be rejected as non-exudate cluster.

This logic is summed up in Table I. $L_1.1$ and $L_2.1$ are shown in brown in Figure 2

TABLE I

IDENTIFYING $L_1.1$ AND $L_2.1$ CLUSTERS

$\max(I)$	$\max(R) - \max(G)$	Possible clusters
maximum	minimum	$\mathbf{L_1.1}$, $\mathbf{L_2.1}$
minimum	X	$L_1.2$, $L_2.2$, $L_1.4$
X	maximum	$L_1.2$, $L_1.3$, $L_2.2$
X	X	$L_1.3$, $L_2.4$, $L_2.3$

Having identified $L_1.1$ and $L_2.1$, their complementary nature is now used to extract the most likely exudate regions. For this we have devised the following scheme:

$L_1.1$ contains slightly over-segmented exudate regions, and several bright background pixels surrounding and including the optic disk. $L_2.1$ contains well-segmented exudates, minute exudates, and several peripheral pixels. The exudate regions can thus be extracted by finding all $L_2.1$ regions present in $L_1.1$, and the other $L_1.1$ regions not present $L_2.1$. Connected components analysis is done to enumerate the

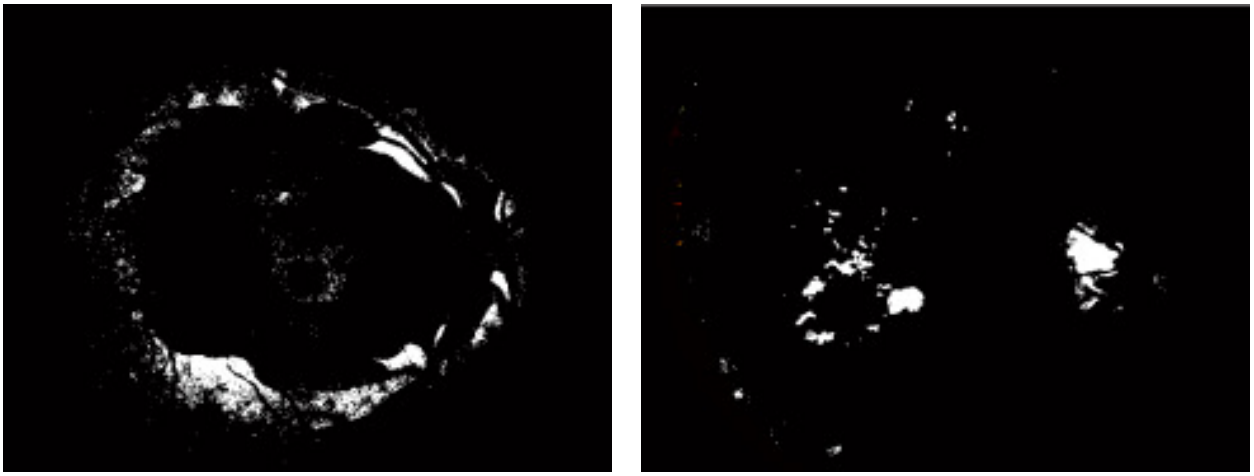

(a) $L_1.1$ regions not present in $L_2.1$ (b) $L_2.1$ regions present in $L_1.1$

Fig. 3. Candidate regions identified by coercing the clusterings

regions and find their presence in $L_1.1$ and $L_2.1$. The desired regions are then extracted, as shown in Figure 3.

Parts of the optic disk and a few bright background regions near it now remain to be identified and suppressed. It can be seen that these superfluous regions are bounded by or cut across by blood vessels. Yet the contrast between the vessels and the candidate region is not prominent, leading to the regions enclosing some vessel segments. The optic disk is one such region, where the major vessels are incident.

We use band decorrelation [10] among the RGB bands in the candidate regions. This results in strong accentuation of the vessel contrast. The red component of the decorrelated result shows a very high value at blood vessels, whereas green component assumes high value at exudates and bright regions (see Figure 4(a)). As per this observation, optic disk regions and regions with vessel crossings assume higher mean decorrelated red value. Thus we find the difference between the mean of red value before and after decorrelation, and suppress candidates yielding a negative value of this difference.

III. Evaluation

A. Dataset

Our method was evaluated against the publicly available DIARETDB1 dataset, consisting of 89 images, of which 38 images contain hard exudates, and 20 contain soft exudates. All images are of same size (1500x1152) and captured using 50 degree field-of-view digital fundus camera [11]. Each ground truth annotation contains polygonal markings of several experts, aggregated to indicate consensus. Against this ground truth we have the possibility of evaluating the segmentation at different consensus levels. We have used the suggested baseline of 75% consensus, and report accuracy of our method in terms of sensitivity and positive predictive value [12] (PPV).

The ground truth is available in terms of polygonal regions, but the polygons are not an exact annotation of the lesion boundary. In order to obtain stricter regions, we performed an automatic thresholding operation in the green band image, restricting the processing to within each annotated polygon (Otsu method was applied for thresholding). Pixels in the polygon having green component above the threshold are used as true exudate regions.

Candidate regions in the segmented image which coincide with the true regions obtained as above, are counted as positive. PPV is found as the ratio of number of positive pixels, to the total number of candidate pixels. Our method achieves a sensitivity of 71.96% and PPV of 87%. For declaring as positive, the degree of coincidence needed between the segmentation and the ground truth is typically set to 50%. This criterion is justifiable considering that several exudates are small, irregular-shaped and appear in clusters, and hence manual annotation by experts is bound to be imprecise.

Applying a region overlap accuracy metric, our approach has an accuracy(recall) of 89.7%. This can be compared with the supervised method of [5], which reports a recall of 87.28% on a dataset of 40 images from a local hospital, and [3], reporting recall of 84.4% at PPV of 62.7% on a set of 50 images. However the performance is lower than [2], reporting 92% recall on a set of 42 images.

IV. Discussion and Conclusions

The use of correlation as distance metric, and use of well-selected feature spaces has compensated for the commonly performed image pre-processing step. To perform clustering, other work in literature have used fuzzy c-means, but have not capitalized on the fuzzy membership values. Moreover, time taken to process a single image is reported to be considerably high (for example, 18 minutes [5] for 752x500 image in Matlab platform) in fuzzy c-means method.

We perform k-means clustering at pixel level using only color information at each pixel, owing to the bottom-up strategy. Processing using a pixel color list data structure enabled much faster clustering (less than 20 seconds on

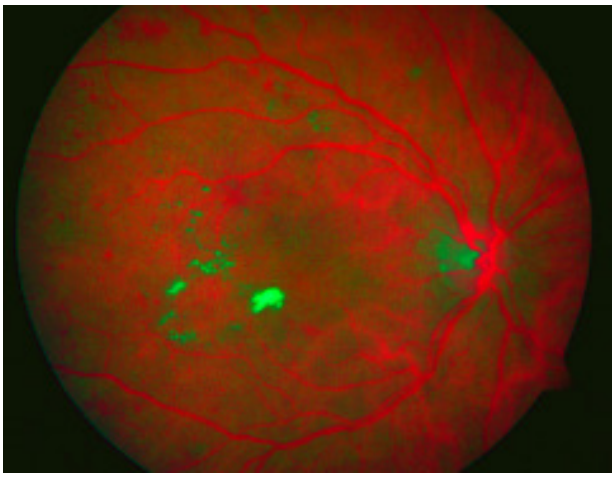

(a) RGB band-decorrelated image

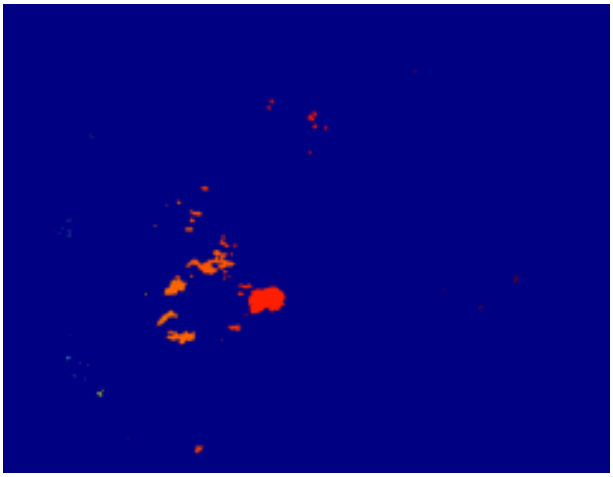

(b) Positive regions after false candidate suppression

Fig. 4. The use of band decorrelation for suppressing optic disk and false candidates

TABLE II
AVERAGE RUNNING TIME FOR A SINGLE IMAGE: 1500X1152, IN MATLAB PLATFORM

Stage	Avg. time taken(sec)
Fundus mask suppression	0.04
Construction of color list	10.51
Color transformations	7.96
Clustering in $\mathbf{f_1}$	12.51
Clustering in $\mathbf{f_2}$	19.48
$L_1.1$ and $L_2.1$ identification	1.282
Coercion of labels	0.302
Suppression of false regions	11.802
Total	63.886

average. See Table II). This comfortably permits clustering on two feature spaces.

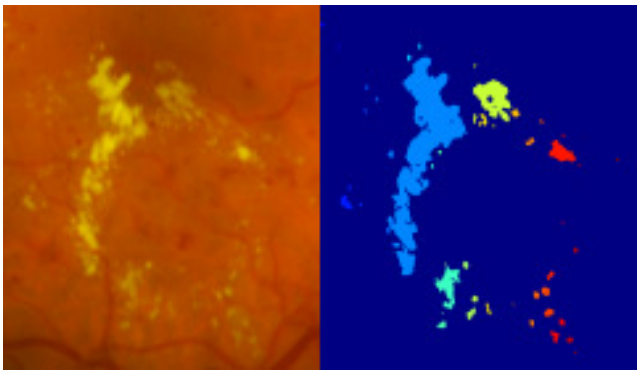

Fig. 5. Sample result: (a) Sub-image, (b) segmented exudates

The high value of PPV indicates that false-positives are few in our approach. Some bright imaging artifacts appearing as small blobs, and laser marks, which appear away from the macula in central views, are two observable false alarms. In few images, exudates appear close to the optic disk, leading to forming a single region enclosing both a true lesion and the optic disk. In this case only parts of the optic disk are suppressed by the method.

Overall, the results obtained indicate that there is good potential for multi-space clustering to be applied as a segmentation technique. Our method is significantly faster than the state of the art, achieves comparable accuracy, and segments are visually well-correlated with the lesion.

REFERENCES

[1] X. Zhang and O. Chutatape, "Top-down and bottom-up strategies in lesion detection of background diabetic retinopathy," in *IEEE Computer Society Conference on Computer Vision and Pattern RecognitionCVPR*, vol. 2, 2005, pp. 422–428.

[2] A. Osareh, M. Mirmehdi, B. Thomas, and R. Markham, *Automatic Recognition of Exudative Maculopathy using Fuzzy C-Means Clustering and Neural Networks*, 2001, pp. 49–52.

[3] M. Garca, R. Hornero, C. I. Snchez, M. I. Lpez, and A. Dez, "Feature extraction and selection for the automatic detection of hard exudates in retinal images," in *Proc. International Conference of the IEEE Engineering in Medicine and Biology Society (EMBS)*, 2007, pp. 4969–4972.

[4] M. Niemeijer, B. van Ginneken, S. R. Russell, M. S. A. Suttorp-Schulten, and M. D. Abrmoff, "Automated detection and differentiation of drusen, exudates, and cotton-wool spots in digital color fundus photographs for diabetic retinopathy diagnosis," *Investigative Ophthalmology and Visual Science*, vol. 48, no. 5, pp. 2260–2267, May 2007.

[5] A. Sopharak, B. Uyyanonvara, and S. Barman, "Automatic exudate detection from non-dilated diabetic retinopathy retinal images using fuzzy c-means clustering," *Sensors*, vol. 9, no. 3, pp. 2148–2161, 2009.

[6] G. B. Kande, P. V. Subbaiah, and T. S. Savithri, "Segmentation of exudates and optic disk in retinal images," in *Proceedings of Indian Conference on Computer Vision, Graphics and Image Processing*, 2008.

[7] M. Amadasun and R. A. King, "Low-level segmentation of multispectral images via agglomerative clustering of uniform neighbourhoods," *Pattern Recognition*, vol. 21, no. 3, pp. 261 – 268, 1988.

[8] S. Bickel and T. Scheffer, "Multi-view clustering," in *Proc. IEEE International Conference on Data Mining (ICDM)*, 2004.

[9] R. Pensa and M. Nanni, "A constraint-based approach for multispace clustering," in *Proceedings of LeGo-08 Workshop (From Local Patterns to Global Models), ECML/PKDD*, 2008.

[10] A. R. Gillespie, A. B. Kahle, and R. E. Walker, "Color enhancement of highly correlated images. i. decorrelation and hsi contrast stretches," *Remote Sens. Environ.*, vol. 20, no. 3, pp. 209–235, 1986.

[11] T. Kauppi, V. Kalesnykiene, J.-K. Kamarainen, L. Lensu, I. Sorri, H. Kalviainen, and J. Pietila, "Diaretdb1 diabetic retinopathy database and evaluation protocol," in *Proc. 11th Conf. on Medical Image Understanding and Analysis*, 2007.

[12] D. G.Altman and J. M. Bland, "Diagnostic tests 2: predictive values," *BMJ*, vol. 309, no. 6947, p. 102, July 1994.